

Evaluation of the Virtual Crystal Approximation for Predicting Thermal Conductivity

Jason M. Larkin¹ and A. J. H. McGaughey^{2,*}

¹*Department of Mechanical Engineering
Carnegie Mellon University
Pittsburgh, PA 15213*

²Department of Mechanical Engineering
Carnegie Mellon University
Pittsburgh, PA 15213

(Dated: December 9, 2012)

In this work, the virtual crystal approximation for mass disorder is evaluated by examining two model alloy systems: Lennard-Jones argon and Stillinger-Weber silicon. In both cases the perfect crystal is alloyed with a heavier mass species up to equal concentration. Phonon properties and thermal conductivity are predicted. These two alloyed systems have different ranges of phonon frequencies, lifetimes, and mean free paths. For Stillinger-Weber silicon, the virtual crystal approximation predicts phonon properties and thermal conductivity in good agreement with molecular dynamics-based methods. For Lennard-Jones argon, the virtual crystal approximation underpredicts the high frequency phonon lifetimes, leading to an underprediction of its thermal conductivity. Resolution of these underpredictions is achieved by considering methods which treat the disorder explicitly.

I. INTRODUCTION

Accurately predicting the thermal conductivity of a dielectric or semiconducting material requires the properties of phonons from the entire Brillouin zone. Accurate predictions of phonon properties for bulk systems can be made with anharmonic lattice dynamics theory using ab initio calculations.⁷⁷⁷⁷⁷⁷⁷⁷⁷⁷⁷⁷ However, computational costs limit the size of computational cells in ab initio calculations to be less than 100 atoms, making it difficult to directly incorporate the effects of disorder.⁷⁷⁷⁷⁷⁷⁷⁷ Alternatively, theory that treats disorder as a harmonic perturbation can be used to estimate the reduction in phonon lifetimes due to disorder scattering without the use of a large unit cell.⁷⁷⁷ Under this approximation, the disordered crystal is replaced with a perfect virtual crystal with properties equivalent to an averaging over the disorder (e.g. mass or bond strength).⁷

Recently, work using ab-initio calculations, anharmonic lattice dynamics (ALD) and the virtual crystal (VC) approximation was used to predict phonon mode frequencies, lifetimes and group velocities of materials with relatively large,[?] moderate,[?], and small[?] thermal conductivities. The use of ALD and VC (referred to as VC-ALD) treats the effects of intrinsic and disorder scattering as perturbations rather than including disorder explicitly.(cite) However, no comprehensive study has been performed to assess the applicability of this perturbative approach for a range of heavily disordered systems using multiple predictive methods.

In intro, mention taud model, VC vs. Gamma point, NMD technique.

The goal of this work is to verify the use of the VC approximation for predicting thermal conductivity by a detailed comparison of 3 predictive methods: MD-based normal mode decomposition (NMD) and green-

kubo (GK), and anharmonic lattice dynamics (ALD) which treats the harmonic and anharmonic phonon scattering as perturbations. When used with the VC approximation, these methods are referred to as VC-NMD and VC-ALD. Two model alloy systems with mass defects ($m_{1-c}^a m_c^b$) are considered: Lennard-Jones (LJ) argon and Stillinger-Weber (SW) silicon. In both cases the perfect crystal is alloyed with a heavier mass species up to equal concentration, spanning a range of perturbative to heavy disorder. These two alloyed systems have very different ranges of phonon frequencies, lifetimes, group velocities and total thermal conductivity. For Stillinger-Weber silicon, VC-ALD predicts thermal conductivity in good agreement with GK. For Lennard-Jones argon, the VC-ALD approximation underpredicts the high frequency phonon lifetimes, leading to an underpredicting of the thermal conductivity. The different thermal conductivity spectra of and the breakdown of the perturbative models are examined.

II. VIRTUAL CRYSTAL (VC) APPROXIMATION

A. Overview

Abeles first introduced the idea of using a virtual crystal (VC) to replace a disordered one, computing the thermal conductivity of Si/Ge alloys by treating both disorder and anharmonicity as perturbations.⁷ Experimentally, Cahill showed that conductivity of dilute Ge-doped Si epitaxial layers agrees with a VC approximation and phonon lifetimes that treat the defects as a perturbation (see section).⁷ Many experimental trends in thermal conductivity of a range of materials can be explained using the VC approximation.(cite) For example, the reduced thermal conductivity of Ge versus Si and

Si/Ge alloys is partly explained by both the increased mass and decreased bulk modulus (stiffness) of the lattice.(cite) Both have the effect of reducing phonon group velocities. (cite) However, a complete description of the thermal transpot in alloys requires modeling intrinsic and disordered scattering to calculate phonon lifetimes (see Section).

Using the VC approximation, we calculate at all compositions of mass variation ($m_{1-c}^a m_c^b$) the phonon modes of the VC (which has a temperature dependent lattice parameter, mass, and force constants of that particular composition) and calculate the frequencies (Section), group velocities (Section), and lifetimes (Section) to predict thermal conductivity (Section). Methods are referred to as VC-ALD (Section) and VC-NMD (Section) use the VC approximation. Explicit disorder is examined in Section (Fig.) and Section (Fig.).

New figure 1: To visually show the VC approximation, how about the following. Make a 4x4 grid of atoms, with two different colors. Put an arrow beside it, pointing to the same 4x4 grid where all the atoms are the same. On the first grid, show the Gamma-point unit cell. On the second grid, show the VC unit cell.

Garg used ab initio calculations with VC-ALD to predict the thermal conductivity of Si-Ge alloys for all concentrations, obtaining good agreement with experiment.[?] Lindsay finds good agreement with experiment for isotopically defected GaN.[?] Both Si-Ge and GaN have relatively large thermal conductivities, even for large concentrations. A detailed study of PbTe(cite) and PbTe/PbSe[?] made predictions for the perfect system in fair agreement with experiment, results which lack for the alloys. The computaitonal studies discussed above were limited to the use of VC-ALD because of the computational cost of ab initio calcualtions. Using empirical potentials, we study the effects of explicit disorder (see Section).

For a perfect system, all vibrational modes are phonons. Using the single-mode relaxation time approximation[?] as an approximate solution of the Boltzmann transport equation[?] gives an expression for thermal conductivity,

$$k_{vib,\mathbf{n}} = \sum_{\kappa} \sum_{\nu} c_{ph}(\kappa) \mathbf{v}_{g,\mathbf{n}}^2(\nu) \tau(\nu). \quad (1)$$

Here, c_{ph} is the phonon volumetric specific heat and $\mathbf{v}_{g,\mathbf{n}}$ is the component of the group velocity vector in direction \mathbf{n} . Since the systems we consider are classical and obey Maxwell-Boltzmann statistics,[?] the specific heat is k_B/V per mode in the harmonic limit where V is the system volume. This approximation is used for all calculations in this work so that direct comparisons can be made for all methods used. Quantify c kB approximation, maybe with reference your SED paper?

Each mode contributing to the thermal conductivity has a frequency $\omega(\kappa)$, which is related to the energy of a phonon in this mode by $\hbar\omega(\kappa)$. In a perfect system,

the allowed energies (frequencies) are the sqaure root of the eigenvalues of the system's Dynamical matrix, $D(\kappa)$, which relates the mode eigenvector ($e(\kappa \alpha)$) and eigenvalue by

$$D(\kappa) e(\kappa \alpha) = \omega(\kappa)^2 e(\kappa \alpha). \quad (2)$$

In a crystal all vibrational modes are plane-waves and as such can be identified by a unique wave-vector κ , eigenvector $e(\kappa \alpha)$, and a possibly degenerate frequency $\omega(\kappa)$. Here, b labels the atom in the unit cell, α label the cartesian coordiantes, and ν labels the mode polarizations. In a crystal, the modes are labled by the allowed wavevector κ and a polarization $\nu = 3b$ which are possibly degenerate in frequency. In a disordered system, such as a crystal lattice with randomly arranged and differing mass species, all vibrational modes exist at the wavevector [000], and $b = N_a$ and $\nu = 3N_a$ where N_a is the total number of atoms in the system. In general, vibrational modes in a disordered system will not be pure plane-waves and will be non-degenerate in frequency. We compare the ordered and disorderd cases in the following section.

B. VC and Gamma DOS Comparison

In this section, we examine the effect of explicit disorder by computing the density of states ($DOS(\omega)$) for vibrational modes of the VC and those of explicitly disordered supercells. Explicitly disordered supercells are generated with atomic positions based on LJ argon's FCC lattice with varying concentrations of randomized masses with composition $m_{1-c}^a m_c^b$. Here, $m^1 = 1$ and $m^2 = 3$ in LJ units. This mass ratio is similar to that of Si and Ge. Disordered supercells are also generated for SW silicon's diamond-FCC lattice using masses of silicon and "heavy" silicon (mass of germanium). Supercells are built cubically with size N_0 , where N_0 refers to the number of repitions of the cubic conventional unit cell in all 3 spatial directions.(cite) Lattices up to size $N_0 = 12$ (LJ argon, 6096 atoms) and $N_0 = 10$ (SW silicon, 8000 atoms).

Equivalent VC lattices are generated using the cubic conventional unit cells of the FCC ($b = 4$) and diamond-FCC ($b = 8$) crystals (where b is the number of atoms in the unit cell). For example, $c = 0.5$ is an LJ VC with average mass of 2. Using appropriate dynamical matrix $D(\kappa)$ (with $\kappa = [000]$ for the supercells), the frequencies are computed using the program GULP.[?] For the VC, the frequencies are identified (up to polarization) by the list of wavevectors allowed by the size of the supercell.(cite)

The DOS calculated for the VC and the explicitly disordered supercells (referred to as Gamma) are shown in Fig. The frequencies agree between VC and Gamma at low frequencies, where the Debye approximation predicts $DOS(\omega) \propto \omega^2$.(cite) The increasing lattice mass (by increasing c) in the VC has the effect of reducing the frequencies. The increasing lattice mass (by increasing c)

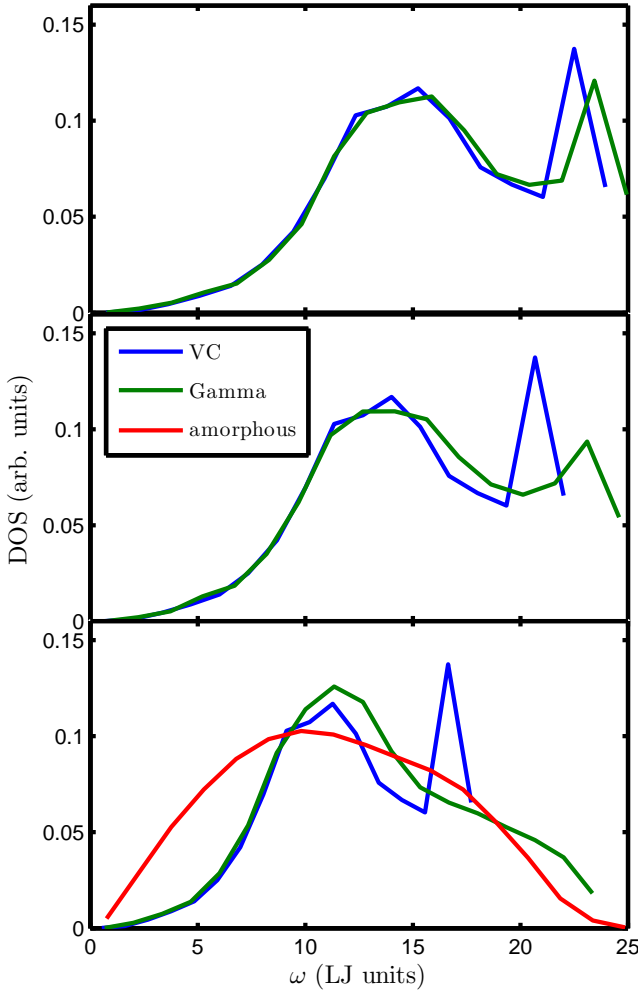


FIG. 1: Fig. 1: $c = 0.5$ vs. amorphous are not really that similar. Does a-Si show any w2 dependence in its DOS?

of Gamma also has the effect of reducing the frequencies. However, the effect of explicit disorder can be seen at high frequencies by a broadening which is more similar to that of the amorphous LJ phase, created using a fast melt-quench process. (cite Shenogin, McGaughey thesis?)

The DOS of the Gamma modes is broadened and shifted to higher frequencies because of the explicit use of atoms of lighter mass than the virtual mass. Similar agreement at low frequencies was found in ab initio predictions for Si_cGe_{1-c} .? Bouchard show that alloy DOS at low frequency varies smoothly with concentration for $a-Si_cGe_{1-c}$.? It is important to note the similarity between the DOS of VC and Gamma at low frequencies and the similarity to the amorphous phase at high frequencies for the heavily disordered system $c = 0.5$, when comparing the phonon lifetimes predicted in Section .

C. Phonon Group Velocities

1. From VC Dispersion

The group velocity vector in a VC is the gradient of the dispersion curves (i.e., $\partial\omega/\partial\kappa$), which can be calculated from the frequencies and wavevectors using finite differences. In this work, the group velocities for the VC are calculated using finite difference and quasi-harmonic lattice dynamics.⁷ The group velocities are necessary to predict the thermal conductivity.

Of particular interest if the phonon mean free path (MFP),(cite)

$$\Lambda(\kappa) = |\mathbf{v}_g| \tau(\kappa), \quad (3)$$

which requires a group velocity. However, predicting an effective dispersion for a disordered system is challenging, while there have been several attempts.(cite Hu, Duda)

2. From Structure Factor of Gamma Modes

Volz and Chen used this method.⁷

Can you provide a physical description of the structure factor?

Measuring the explicitly disordered mode's structure factor is a method to test for the plane-wave character of modes at a particular wavevector and polarization.(cite) The structure factor is defined as

$$S^{L,T}(\kappa) = \sum_{\nu} E^{L,T}(\nu) \delta(\omega - \omega(\nu)), \quad (4)$$

where E^T refers to transverse polarization and is defined as

$$E^L(\kappa) = \left| \sum_{l,b} \hat{\kappa} \cdot e(\kappa \cdot \alpha) \exp[i\kappa \cdot \mathbf{r}_0(l)] \right|^2 \quad (5)$$

and E^L refers to longitudinal polarization and is defined as

$$E^T(\kappa) = \left| \sum_{l,b} \hat{\kappa} \times e(\kappa \cdot \alpha) \exp[i\kappa \cdot \mathbf{r}_0(l)] \right|^2. \quad (6)$$

Here, $\mathbf{r}_0(l)$ refers to the lattice position in the disordered supercell labeled using the VC unit cell with atom b in the l unit cell, which are ordered even in the disordered supercells. Explicit disorder is accounted for in the mode frequencies $\omega(\kappa)$ and eigenvectors $e(\kappa \cdot \alpha)$ which are calculated with $\kappa = [000]$.

With increasing concentration, the structure factor spreads in width, particularly at high frequencies. As the

lattice VC mass becomes larger, the peaks in the structure factor shift to lower frequencies. The peaks in the structure factor for Gamma point modes are shifted to slightly higher frequencies because of the explicit use of masses $m^a = 1$ less than the VC mass, and effect which can also be seen in the DOS comparisons (Section , Fig).

An effective dispersion can be extracted by locating the peaks in the structure factors, where the effects of polarization, virtual mass, and anisotropic dispersion can be observed (Fig.). In ordered systems, the group velocity generally scales with the density (lattice mass).(cite) Thus, for alloys, there should also be a corresponding scaling of the group velocity with the alloy's concentration (lattice mass). This can be observed as the peaks in the structure factor are reduced in frequency from $c = 0.0$ to $c = 0.5$. Also demonstrated is the importance of dispersion along different lattice directions ([100], [111]) and polarizations (S^L, T).

Well-defined peaks at all wavevectors is unique to the disordered lattice. Typically, the structure factor for amorphous materials has well-defined peaks only for small wavevector.(cite)

Predict lifetime from DSF, compare to Ioffe-Regel limit.

The frequencies extracted from the structure factors agree with the VC predictions to less than 5% at the highest frequencies. Because of this, we use the group velocities predicted by the VC dispersion in both our VC-NMD and VC-ALD calculations for consistency and simplicity.

Duda shows the reduction in group velocity of moderate to high frequency modes in a 1D alloy are drastically reduced by considering the effects of zone folding.[?] Based on the structure factors in Fig. , the reduction due to zone folding seems to underpredict the group velocity of moderate to high frequency modes. Ambiguity can be resolved by considering the thermal diffusivity of a given mode, which incorporates the variation of both group velocity and lifetime (see Section).

D. Phonon Lifetimes

E. From VC-NMD and Gamma

As an alternative to the VC-ALD models for predicting phonon lifetimes (Eq. and , Section), we use the normal mode decomposition (NMD) method.(cite) NMD maps the atomic coordinates (position and velocities) of all atoms in an MD simulation onto vibrational normal modes.(cite) The MD simulation is performed using the disordered supercells so that the effects of explicit disorder are considered. The vibrational mode frequencies ($\omega(\kappa)$) and eigenvectors ($e(\kappa_\alpha^b)$) are necessary for the mapping. The vibrational normal mode coordinates, $q(\kappa; t)$ and $qdot(\kappa; t)$, are required to calculate the total vibrational normal mode energy $E(\kappa)(t)$.

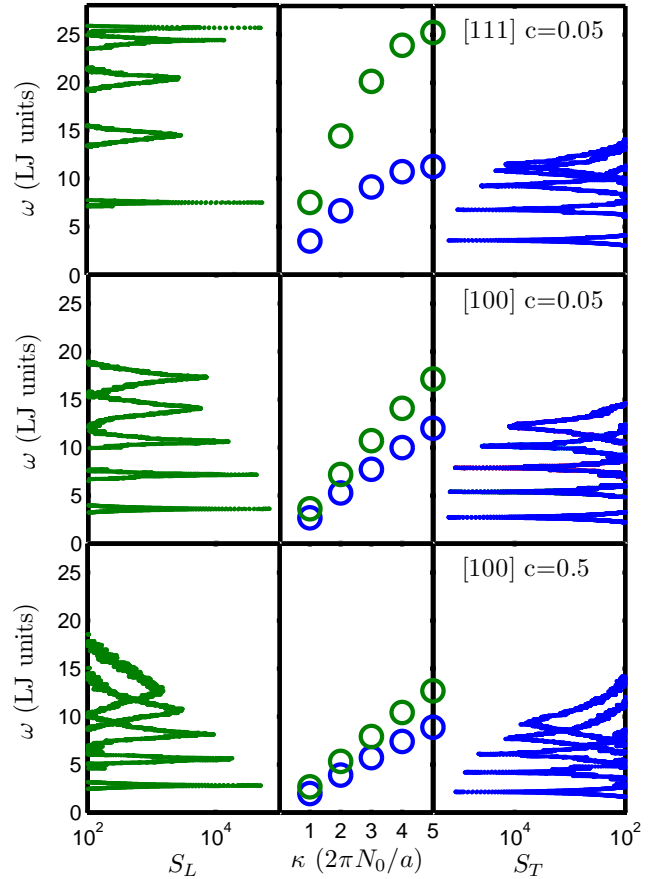


FIG. 2: virtual crystal results

The lifetimes are predicted using the frequencies and eigenvectors from both the VC ($\omega(\kappa), e(\kappa_\alpha^b)$) and the Gamma supercell ($\omega(\kappa), e(\kappa_\alpha^b)$ with $\kappa = [000]$). The phonon lifetime is predicted using

$$\tau(\kappa) = \int_0^\infty \frac{\langle E(\kappa; t) E(\kappa; 0) \rangle}{\langle E(\kappa; 0) E(\kappa; 0) \rangle} dt. \quad (7)$$

This is necessary for the disordered systems where spectral NMD can produce multiple peaks in an isolated mode's energy spectrum. This feature is not surprising given two considerations: 1) the MD simulations contain explicit disorder which influences the atomic trajectories 2) the normal modes are mapped without using the exact eigenvectors and frequencies of the explicitly disordered system (see Fig. and).

Under the VC approximation, the phonon eigenvectors are those of pure plane-waves by definition. In a disordered supercell, the vibrational modes are not pure plane-waves (phonons) (see Section) and exist at the Gamma point ([000]). Lifetimes predicted using VC-NMD and the Gamma supercells, are examined in the next section.

Extra noise in Gamma due to no symmetry averaging. The lifetimes predicted using the VC approximation

and the Gamma supercells are shown in Fig.

eigenvector mappings^{7, 8} use NMD to predict the phonon properties of PbTe using a classical model.⁹ half-huesler uses Φ' and ALD, find good agreement.⁷ finds increased scattering in water-filled CNTs.⁷ finds increased scattering of phonons in CNTs on a substrate.

In these studies, the atomic coordinates are being mapped onto modes which are not eigenmodes of the system's Hamiltonian. Still, the spectral widths (inverse lifetimes) of these mappings contain information about the scattering time scales associated with these modes.

Previous studies have used the spectral NMD using exact and non-exact mode eigenvectors to extract mode timescales.(cite) The lifetimes using these mappings contain the effects of both intrinsic(cite) and disorder scattering(cite). Interpretation of these timescales as phonon lifetimes has led to successful thermal conductivity predictions in a range of ordered and disordered materials. (cite) Given the possible ambiguity of the lifetimes predicted using VC-NMD, it is necessary to compare the predicted thermal conductivities using a range of methods which posses no such ambiguity (such as VC-ALD and GK, see Section).

A general statement from statistical physics^{16,17} also imposes the mode energy autocorrelation to decay exponentially with the relaxation time k .⁷

F. From VC-ALD

Assuming the initrinsic and disorder scattering mechanisms to operate independently, the effective phonon lifetime can be found using Matthiesen's rule(cite),

$$\frac{1}{\tau(\kappa)} = \frac{1}{\tau_{p-p}(\kappa)} + \frac{1}{\tau_d(\kappa)}, \quad (8)$$

where $\tau_{p-p}(\kappa)$ accounts for phonon-phonon scattering, accounts for boundary scattering, $\tau_d(\kappa)$ accounts for defect scattering.

Phonon-phonon scattering ($\tau_{p-p}(\kappa)$) is typically treated using anharmonic perturbation theory (ALD) including only 3-phonon processes.^{7, 8, 9} It has been estimated that the effects of higher order phonon processes are small⁷, particularly at low temperatures.⁷ At low frequencies, $\tau_{p-p}(\kappa)$ follows a scaling due to both normal ($B_1\omega^2$) and umklapp ($B_2\omega^2$) 3-phonon scattering processes, where the density of states is Debye-like. The constants B_1 and B_2 are typically fit to experimental data.

Using harmonic perturbation theory, Tamura gives a general expression for mass point defect scattering?

$$\frac{1}{\tau_d(\kappa)} = \frac{\pi}{2N}\omega(\kappa)^2 \sum_{\kappa' \kappa'} \delta(\omega(\kappa') - \omega(\kappa')) \sum_b g(b) |e^*(\kappa' \cdot b) \cdot e(\kappa \cdot b)|^2, \quad (9)$$

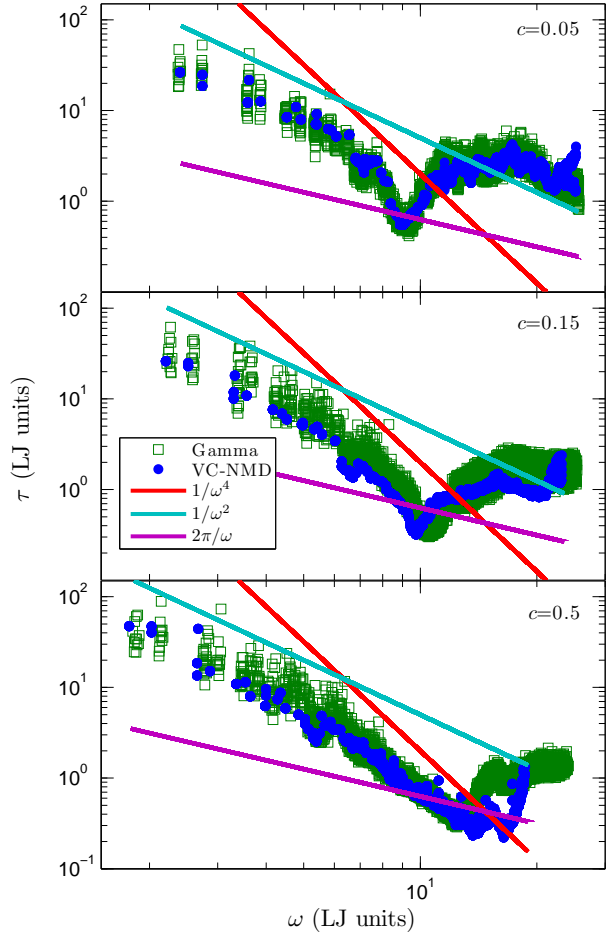


FIG. 3: virtual crystal results

where $g(b) = \sum_i c^i(b)(1 - m^i(b)/\bar{m}(b))^2$, N is the number of unit cells. and c^i is the fraction, $m^i(b)$ is the mass, and \bar{m}_i is the average mass of the i-th species. In this work, binary alloys are considered with m_{1-c}^1 and m_c^2 . The

For the simple binary alloys considered in this work, the species

$$\frac{1}{\tau_d(\kappa)} = \frac{\pi}{2} g \omega(\kappa)^2 D(\omega(\kappa)), \text{ where } D(\omega(\kappa)) \text{ is the density}$$

of states. Under the Debye-approximation, the phonon scattering due to mass point-defects is given by $A\omega^{-4}$, where A is a constant related to the unit cell volume, branch-averaged group velocity, and disorder coupling strength (g in Eq. above). The frequency dependence (ω^4) is the same as Rayleigh scattering, which is valid at low frequency where the Debye approximation is valid.

Bond disorder can be accounted for using a similar expression with an average atomic radius or suitable scattering cross-section.^{7, 8} The effect of bond and mass disorder has been investigated computationally by Skye and Schelling for Si/Ge⁷, where it was shown that mass disorder is the dominant scattering mechanism. In this work we consider only mass disorder.

While the expression for harmonic defect scattering (Eq.) is valid for perturbative disorder, its use leads to good agreement with several experimental and computational results with large disorder. Cahill shows that conductivity reduction in dilute Ge-doped Si epitaxial layers is captured by mass perturbative disorder.⁷ In this case, the mass disorder is large ($m_{Ge}/m_{Si} = 2.6$) but the overall disorder strength is dictated by the concentration. For example, as little as $6.2 \times 10^{19} \text{ cm}^{-3}$ Ge ($g = 3.1 \times 10^{-3}$) is enough to reduce the thermal conductivity of Si by almost a factor of 2.⁷ Even in the case of the $Ni_{0.55}Pd_{0.45}$ alloy, the atomic species are chemically similar but both the mass disorder ($m_{Pd}/m_{Ni} \approx 2$) and concentration are large ($g = 0.078$) and good agreement is seen with the Eq. .⁷

Computational results for moderate to high thermal conductivity alloys show good to excellent agreement with experimental results^{7, 8, 9}. Computational results for small thermal conductivity alloys show some universal trends but little experimental results are available for comparison.⁷ However, a comprehensive validation has not been performed.

For the VC-ALD method, the intrinsic $\tau(\kappa)_{p-p}$ is calculated using the method described in.⁷ To calculate the disordered lifetimes $\tau(\kappa)_d$ (Eq.), it is necessary to broaden the δ function using a Lorentzian function. For all calculations, the Lorentzian was broadened using a value of 100 times the mean level spacing. For the system sizes here, the results do not differ significantly if this broadening value is varied by changing it manually or making the system size (N_0) bigger.

G. Vibrational Mode Diffusivity Limit

In the classical limit, where the specific heat $c_p(\kappa) = k_B$, a vibrational mode's contribution to thermal conductivity is determined by the mode thermal diffusivity. For phonons, the thermal diffusivity is simply

$$D_{ph}(\omega(\kappa)) = v_g^2(\kappa) \tau(\kappa). \quad (10)$$

In heavily disordered systems, such as large c alloys or glasses, modes can transport heat by harmonic coupling due to the disorder in the Allen-Feldman (AF) theory.(cite) With sufficient disorder, the harmonic AF theory is capable of accurately predicting a finite thermal conductivity.(cite shenogin, FKA)

We now compare the phonon mode diffusivities, $D_{ph}(\omega(\kappa))$ predicted by both VC-NMD and VC-ALD to the proposed lower limit $D_{AF,HS} = (1/3)v_s a$ (see Section). Here, a is 1/2 the lattice constant of the cubic conventional unit cells used for both FCC LJ argon and diamond-FCC SW silicon, although the choice of this length scale is not unique. For the a value in Eqs. (12)-(14), why not use the bond length?

For LJ argon, VC-NMD predicts lifetimes which are generally larger than the period ($2\pi/\omega(\kappa)$) of the vibra-

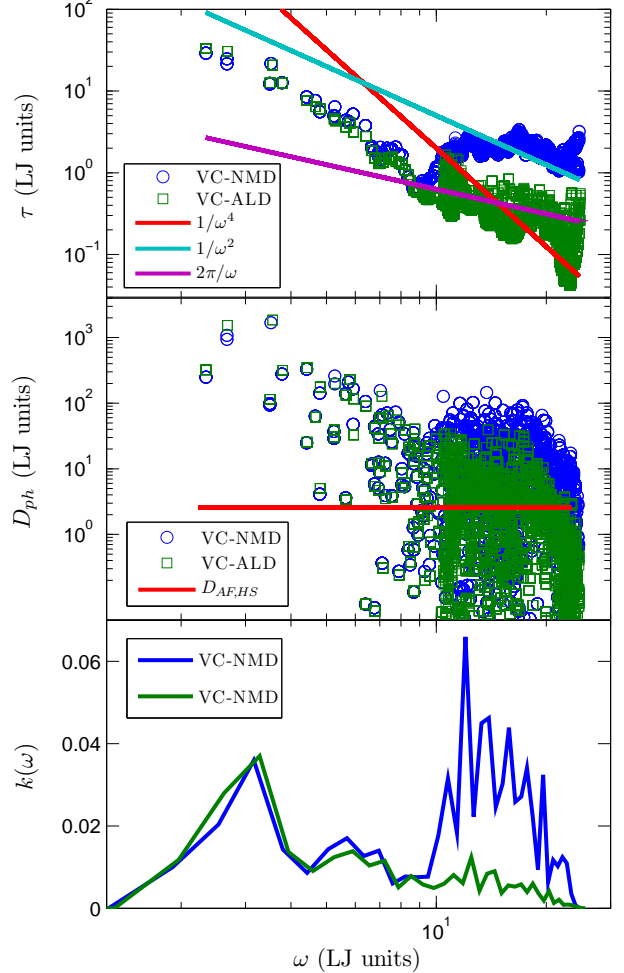


FIG. 4: gamma point results

tional oscillation (Ioffe-Regel limit)(cite), and actually increase high frequency for small intervals (Fig. and). VC-NMD predicts larger phonon lifetimes at high frequency compared to VC-ALD (Fig.), which predicts essentially monotonically decreasing lifetimes with increasing frequency. Because VC-NMD and VC-ALD use the same values for $v_g(\kappa)$, the phonon mode diffusivities D_{ph} are also underpredicted by VC-ALD compared to VC-NMD. This leads to an underprediction for VC-ALD of both the thermal conductivity spectrum (Fig.) at high frequency and the total thermal conductivity (Fig.) compared to VC-NMD.

For both VC-NMD and VC-ALD, a significant number of modes have $D_{ph}(l; t) D_{AF,HS}$. This leads to an underprediction of the total thermal conductivity compared to GK (Fig.). The diffusivity of these modes can be adjusted such that any mode with $D_{ph}(l; t) D_{AF,HS}$ is given $D_{ph} = D_{AF,HS}$. The result of this adjustment, referred to as VC-NMD* and VC-ALD*, is examined in the next section.

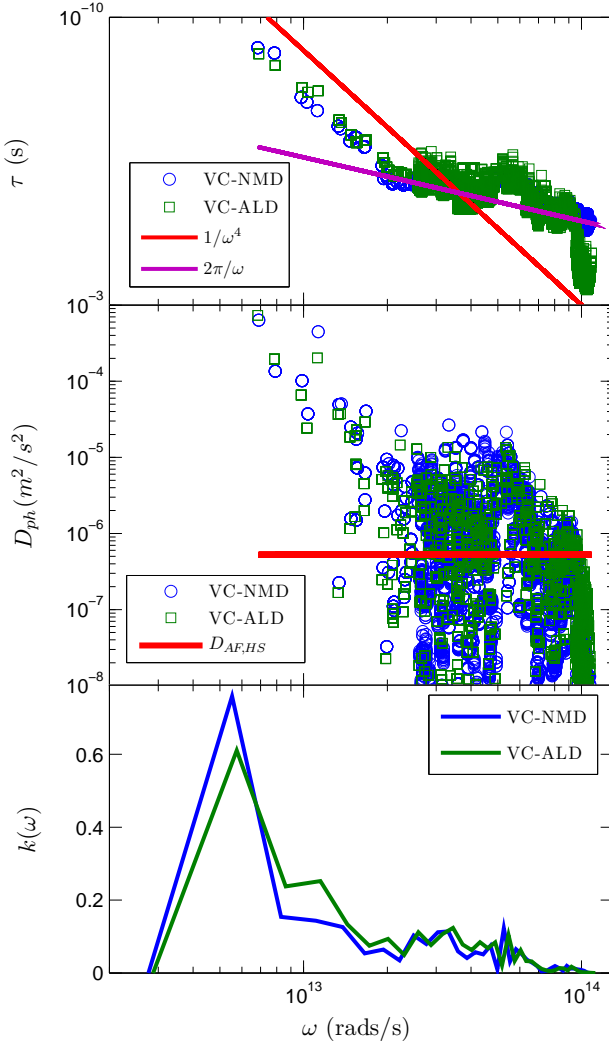


FIG. 5: gamma point results

In the classical limit, the AF thermal conductivity is written as

$$k_{AF} = \sum_{\omega} \frac{k_B}{V} D_{AF}(\omega), \quad (11)$$

where V is the system volume and $D_{AF}(\omega_{AF})$ is the thermal diffusivity of the mode labeled by frequency $\omega_{AF} \equiv \omega_{\nu}$, with ν ranging over all modes in the supercell and $\kappa = [000]$.^(cite)

In the high-scatter (HS) limit,^(cite) the AF diffusivity of each mode is

$$D_{AF,HS} = \frac{1}{3} v_s a. \quad (12)$$

A similar HS limit for mode diffusivity is given by the Cahill-Pohl (CP) model,

$$D_{CP,HS} = 0.403 v_s a. \quad (13)$$

The CP thermal conductivity prediction in the HS limit

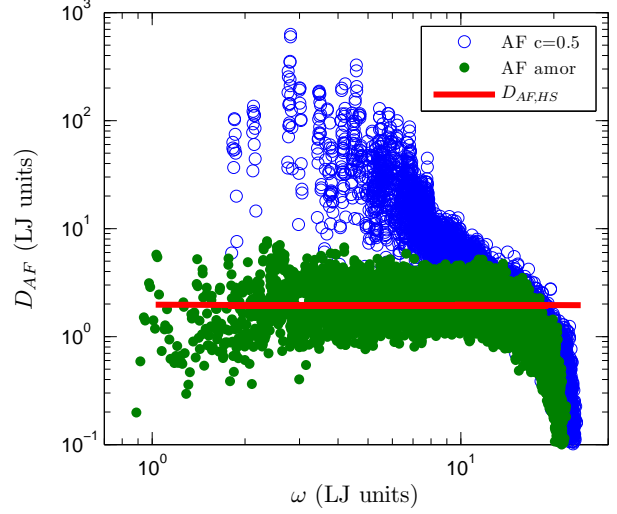


FIG. 6: gamma point results

is

$$k_{CP,HS} = \left(\frac{\pi}{6}\right)^{1/3} \left(\frac{3}{2}\right) \frac{k_B}{V_b} b v_s a, \quad (14)$$

where V_b is the volume of the unit cell, v_s is the branch-averaged sound speed, and a is the lattice constant (or appropriate length scale).⁷ Comparing with Eq., the AF,HS limit predicts a mode diffusivity and thermal conductivity which is %20 smaller than CP,HS.⁷ Ignoring this small difference, the interpretation for both $D_{AF,HS}$ and $D_{CP,HS}$ is of a vibrational mode with a group velocity equal to the sound speed and mean-free path equal to the lattice spacing. While the CP,HS model assumes $\tau = 1/\omega$ and $v_g = v_s$ for all modes, the AF theory is capable of predicting the mode diffusivities without any assumptions other than a harmonic approximation.^(cite)

While the frequency spacings in a finite system limit the D_{AF} of the lowest frequency modes, in the infinite-size, low-frequency limit, the AF conductivity of a disordered lattice is divergent due to lack of anharmonic phonon-phonon scattering.^(cite) While the low frequency modes are not treated properly in the harmonic AF theory, D_{AF} of high frequency modes in the heavily disordered ($c = 0.5$) LJ alloy approaches that of similar frequency modes in the amorphous phase (Fig.). In the amorphous phase, modes with significant contribution to thermal transport can be modeled using a mode-independent diffusivity of $D_{AF,HS}$ (Eq.). In fact, the difference between $k_{AF} = 0.099 W/m = K$ and $k_{HS,CP} = 0.124$ is approximately %20. This places a plausible lower-bound on the value of the phonon mode diffusivities, $D_{ph} \geq D_{AF,HS}$, predicted by VC-NMD and VC-ALD in the following section.

III. THERMAL CONDUCTIVITY PREDICTIONS

An addition of as little as 10% Ge is sufficient to reduce the thermal conductivity to the minimum value achievable through alloying. Theoretically, mass disorder is found to increase the anharmonic scattering of phonons through a modification of their vibration eigenmodes. Notably, the thermal conductivity is found to drop sharply after only a small amount of alloying. This is due to the strong harmonic scattering of phonons even in the dilute alloy limit.

Duda shows that taking a perfect alloy and disordering via an order parameter allows control of thermal conductivity.⁷

In fact, the beginning breakdown of the intrinsic scattering model ($\tau_{p-p}(\kappa)$) can be observed for the perfect ($c = 0.0$) crystal at $T = 40$ K (see Fig.), where ALD begins to overpredict compared to GK. This can be explained by the emerging importance of higher order ($n > 3$) n-phonon process at high temperatures.⁷

For LJ argon, bulk thermal conductivity predictions are made for VC-NMD, VC-ALD and GK (Fig.). For SW silicon, bulk thermal conductivity predictions can only be made for VC-ALD and GK (see Appendix). For LJ argon, both VC-NMD and VC-ALD underpredict the thermal conductivity compared to GK. By adjusting

Experimental measurements of isotopically pure and Ge-doped Si epitaxial layers demonstrate the original theory by Abeles can predict thermal conductivity in dilute alloys. Abeles also found good agreement with dilute predictions for both experimental measurements of both Si-Ge alloys and also (Ga,In)As alloys.⁷ However, both of these alloy systems have a relatively high thermal conductivities (on the order of 1-10 W/m-K at 300 K). However, in the heavily disordered system In(As,P) (mass ratio of 3.7) worse agreement with the Abeles theory is observed.

The theory by Tamura is able to treat disorder scattering in an arbitrary crystal with dispersion. The theory, however, fails to predict the lifetimes of high-frequency modes, which are critical to the total thermal conductivity in LJ argon (see Fig. and). To match the predicted phonon lifetime at high frequency for $c = 0.05$ ($\tau(\kappa) \propto \text{const.}$, Fig.), the Tamura theory requires a DOS which scales as $D(\omega(\kappa)) \propto \text{const.}$. Clearly from Fig. , this is not the case with either the VC or Gamma modes. To match the predicted phonon lifetime at high frequency for $c = 0.5$ ($\tau(\kappa) \propto 1/\omega(\kappa)$, Fig. , also true for all c in SW silicon),

While Broido found that omission of optical scattering overpredicts the thermal conductivity of bulk Si by a factor of 2-3, optical modes contribute less than 5% to thermal conductivity itself. Similarly, the diffusivity adjusted thermal cobductivities of SW Si are increased by less then 5%, demonstrating the unimportance of the high frequency “optical” modes in SW Si alloys.

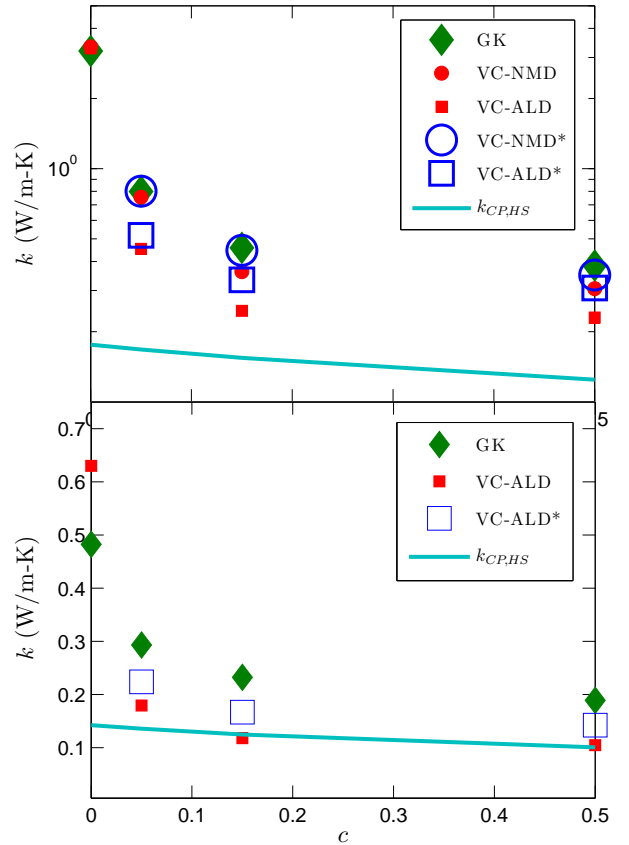


FIG. 7: The vibrational conductivity of LJ alloys predicted using MD simulations and the Green-Kubo method. The predicted thermal conductivities are for a LJ alloy of the form $m_1^a m_c^b$, where $m^a = 1$, $m^b = 3$, and $m_r = m^a/m^b = 3$ (in LJ units). As the alloy concentration is increased perturbatively, the vibrational conductivity drops quickly and saturates to a minimum at $c = 0.5$. For $c = 0.5$ the system is heavily disordered and the vibrational conductivity approaches that of an amorphous system.

IV. DISCUSSION

the problem is with taud. VC-NMD agrees well with GK for both LJ and SW, while ALD-taud underpredicts for LJ. VC-NMD and ALD-taud use the same group velocity and classical specific heat.

Particularly challenging is predicting a representative group velocity for modes in a disordered systems. Use of the VC approximation is a theoretically and computationally simple way to predict a representative group velocity.

High thermal conductivity materials tend to have a conductivity spectrum which is peaked in the low frequency range.(cite) It is in this range where the mode lifetimes follow closely the scalings with frequency which can be predicted by treating intrinsic and disorder scattering as perturbations (Eq.).

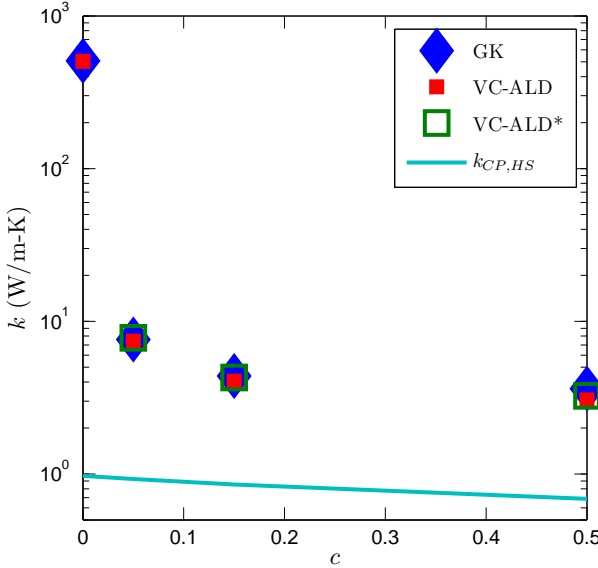


FIG. 8: The vibrational conductivity of LJ alloys predicted using MD simulations and the Green-Kubo method. The predicted thermal conductivities are for a LJ alloy of the form $m_{1-c}^a m_c^b$, where $m^a = 1$, $m^b = 3$, and $m_r = m^a/m^b = 3$ (in LJ units). As the alloy concentration is increased perturbatively, the vibrational conductivity drops quickly and saturates to a minimum at $c = 0.5$. For $c = 0.5$ the system is heavily disordered and the vibrational conductivity approaches that of an amorphous system.

In contrast, in LJ argon the high frequency phonon mode properties are critical to the thermal transport.(cite) While the low frequency phonon properties predicted by VC-NMD and VC-ALD agree, it is the failure of the perturbative models at high frequency which causes VC-ALD to underpredict. The failure to account for harmonic disordered scattering due to the AF theory is responsible for causing both VC-NMD and VC-ALD to underpredict versus GK, which affects the high frequency modes significantly. LJ argon, with lower frequencies, lifetimes, and group velocities compared to “stiff” SW silicon, is considered a “soft” system. The predictions using VC-NMD, VC-ALD demonstrate the importance of explicit disorder modeling in “soft” systems and possible underprediction of the thermal properties.[?]

For SW silicon, the low frequency modes dominate thermal transport even in the heavily disordered alloy.(cite new Hopkins) It is thus unsurprising that predictions for SW silicon using VC-ALD agree well with VC-NMD and GK. This is also a plausible explanation for the success of predictions using VC-ALD and ab initio calculations compared to experiment for “stiff” systems (i.e. Si-Ge, GaN, and Diamond).(cite)

In SW silicon even the amorphous phase has significant contributions from propagating modes which can be considered to be phonons. This is can seen by compar-

ing the thermal conductivity predicted for the SW silicon amorphous phase ($k_{GK} = 3 \text{ W/m-K}$ (cite)) compared to $k_{CP,HS} = 0.5 \text{ W/m-K}$. For LJ argon in the amorphous phase, $k_{GK} = 0.121 \text{ W/m-K}$ and $k_{CP,HS} = 0.12 \text{ W/m-K}$, indicating that all important modes to thermal transport are non-propagating.

V. SUMMARY

Appendix A: Finite Simulation-Size Scaling for Thermal Conductivity

To predict a bulk thermal conductivity, extrapolation is used by the following finite size scaling $1/k \propto 1/N_0$. For VC-NMD and VC-ALD, the criteria for the validity of this finite size scaling is the low frequency modes in the finite system must be dominated by intrinsic scattering such that $\tau(\kappa_\nu) \propto \omega(\kappa_\nu)^{-2}$ and approximately follow the Debye approximation with respect to $v_{g,n}$ and DOS $D(\omega(\kappa_\nu))$.(cite) For LJ argon, this requirement is satisfied for modest system sizes (up to $N_0 = 10$) so that both VC-NMD and VC-ALD predictions can be extrapolated to a bulk value. For SW silicon, the thermal conductivity is dominated by low-frequency modes. Because of this, large system sizes (up to $N_0 = 24$) are needed to satisfy the extrapolation requirement and only VC-ALD can be used.(cite) This underlines the computational efficiency of the VC-ALD method which is necessary when computationally expensive ab initio methods are used. (cite) For the GK method, the finite size extrapolation is used for both LJ argon and SW silicon for smaller system sizes $N_0 \leq 12$. The validity of this result can be explained in terms of a combination of effects which are specific to the MD simulations.[?]

